

# ELECTRON CLOUD ESTIMATES FOR THE JEFFERSON LAB EIC

K. E. Deitrick\*, V. S. Morozov, T. Satogata,  
Thomas Jefferson National Accelerator Facility, Newport News, VA 23606, USA

## Abstract

In this work, we present preliminary estimates for electron cloud build-up and saturation for the ion ring of the Jefferson Laboratory Electron-Ion Collider (JLEIC) currently under development. Using the baseline ion ring design, we study the impact of various operational parameters on the behavior of the electron cloud for a 100 GeV proton beam, including estimated tune shifts.

## INTRODUCTION

The Jefferson Lab Electron-Ion Collider (JLEIC) [1], shown in Fig. 1, currently under development anticipates a high luminosity - which requires careful consideration of various collective effects, including electron cloud. The build up of the electron cloud in an ion machines is seeded by primary electrons, which typically originate from three causes - photoelectrons, ionization of residual gas, and electrons produced by collisions between the beam pipe and stray particles. This paper serves as a current evaluation of the severity of electron cloud in the current JLEIC design, using the simulation code PyECloud [2].

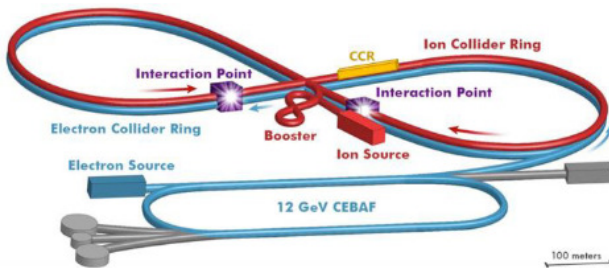


Figure 1: A conceptual layout of JLEIC.

## SIMULATION SET UP

Using PyECloud, it is possible to observe the density of electrons over time for a given set of proton beam, vacuum, and secondary electron yield (SEY) parameters, which are given in Table 1. The SEY settings assume that the beam pipe is made from stainless steel [4]. These parameters were used to simulate the electron density for a number of cases, including dipoles, drifts, quadrupoles, and sextupoles. These cases are summarized in Table 2. For the quadrupoles and sextupoles, the highest field gradient outside of the interaction region (IR) magnets is used - these are not representative of the average field for these elements.

Table 1: Proton Beam and Vacuum Parameters Used in the simulations

Parameter	Symbol (Unit)	Value
Beam energy	$E_b$ (GeV)	100
Circumference	$C$ (m)	2230
Collision frequency	$f_c$ (MHz)	476
Beam pipe cross-section	-	Circular [3]
Beam pipe radius	$r_b$ (mm)	40 [3]
Number of bunches per train	$K_B$	1856
Bunch spacing	$s_b$ (ns)	2.1
Bunch population	$N_p$ ( $10^{10}$ )	0.98
Bunch length	$\sigma_l$ (cm)	1
Bunch profile	-	Gaussian
Empty bunches between trains	-	126
Normalized emittance	$\epsilon_x^N, \epsilon_y^N$ ( $\mu\text{m}\cdot\text{rad}$ )	0.5, 0.1
Residual gas pressure	$P$ (nTorr)	5
Temperature	$T$ (K)	4.5
Peak SEY	$\delta_{max} \equiv \delta(E_{max})$	2.25
Ionization cross-section	$\sigma_i$ (Mbarns)	2
Energy at peak SEY	$E_{max}$ (eV)	300

Table 2: Magnetic Properties for Simulations

Element	Absolute Field Strength	Unit
Drift	-	-
Dipole	3.06	T
Quadrupole	85	T/m
Sextupole	450	T/m <sup>2</sup>

## RESULTS FOR DIFFERENT ELEMENTS

The electron cloud density for each magnetic element is shown in Fig. 2 over the time span of a single bunch train, which contains 1856 bunches separated by 2.1 ns. Simulations have been performed for multiple bunch trains in dipoles and drifts, separated by 126 empty buckets, and the electron cloud density behavior remains consistent despite the bunch train number - the electron cloud reaches saturation before the end of the bunch train and decreases in the gap between trains. For certain elements, like the sextupole, the preceding bunch train will mean that successive trains reach saturation more quickly. This behavior can be seen

\* deitrick@jlab.org

in the electron cloud density within the drift and sextupole over two bunch trains shown in Fig. 3. While the time to saturation in the drift is comparable between the first and second train for the drift, the time to saturation in the second bunch train of the sextupole is quicker than in the first

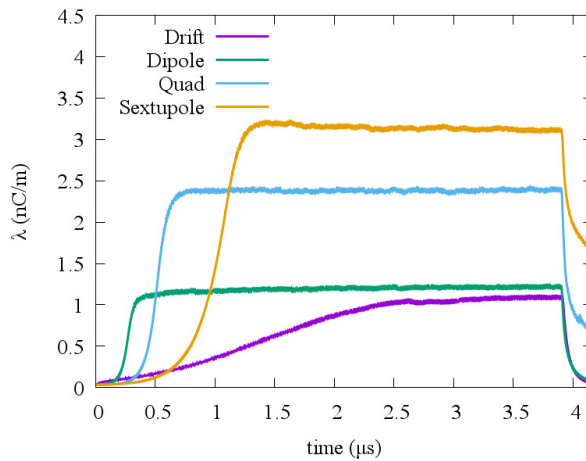


Figure 2: Electron cloud line density over a bunch train (1856 bunches, followed by 126 empty buckets) for various elements and a drift.

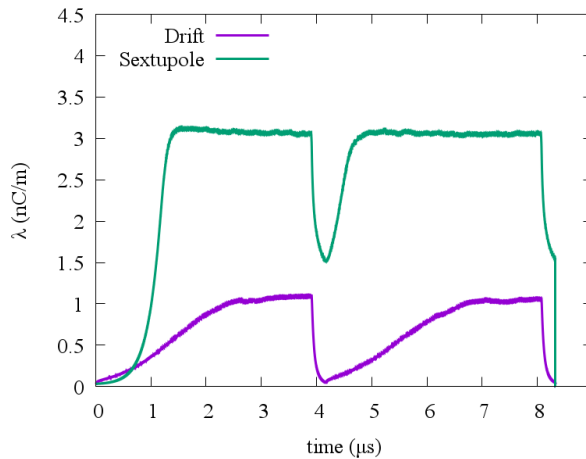


Figure 3: Electron cloud line density over two bunch trains (1856 bunches, followed by 126 empty buckets in each) for a sextupole and a drift.

Using these results, it is possible to calculate the estimated horizontal tune shift per unit length with the formula

$$\Delta\nu_x/L = \frac{r_p \bar{\beta}_x \rho_e}{2\gamma_b} \quad (1)$$

where  $r_p = 1.535 \times 10^{-18}$  m is the classical proton radius,  $\rho_e$  is the electron cloud density,  $\bar{\beta}_x = 49$  m is the average horizontal beta function, and  $\gamma_b = 106.6$  is the typical relativistic factor of the proton beam. The formula for the estimated vertical tune shift per unit length is similar, simply replacing  $\bar{\beta}_x$  with  $\bar{\beta}_y$ , which is 66 m. Taking  $L$  to be 2230 m,

Table 3: Simulation Results for Different Magnetic Elements

Element	$\lambda_e$ (nC/m)	$\rho_e$ ( $\text{m}^{-3}$ )	$\Delta\nu_x$ ( $10^{-3}$ )	$\Delta\nu_y$ ( $10^{-3}$ )
Drift	1.09	$1.36 \times 10^{12}$	1.06	1.43
Dipole	1.23	$1.53 \times 10^{12}$	1.20	1.62
Quadrupole	2.40	$2.99 \times 10^{12}$	2.34	3.16
Sextupole	3.11	$3.87 \times 10^{12}$	3.03	4.10

Table 4: SEY Parameters Corresponding to Different Materials

Material	$\delta_{max}$	$E_{max}$ (eV)	$\sigma_i$ (Mbarns)
Stainless steel [4]	2.25	300	2
Copper [4]	1.90	300	2
Partially scrubbed copper [5]	1.55	125	2

the circumference of the ion ring, we can estimate the vertical and horizontal tune shift per turn - these results are given in Table 3. All of the estimated tune shifts per turn fall below  $4.5 \times 10^{-3}$ , which does not indicate that electron cloud effects will have a significant impact on the performance of the machine. This is particularly true as taking the highest possible density and assuming it for the entire circumference leads to overestimation.

## RESULTS FOR DIFFERENT SEY PROPERTIES

Thus far, we have assumed that the beam pipe is made from stainless steel. However, it is suitable to evaluate the electron cloud density for different materials, to evaluate the impact of SEY parameters. The three chosen materials are stainless steel, copper [4], and partially-scrubbed copper [5]. The SEY parameters of the three materials are given in Table 4.

Using these parameters, we have simulated the electron cloud density for two successive bunch trains for the three different materials in the dipoles; the electron cloud density as a function of time for each of the three materials is shown in Fig. 4. Using the same approach as in the previous section, it is possible to estimate the tune shift for the electron cloud density assuming different materials. The results of these calculations are given in Table 5. While it is clear that copper out-performs stainless steel, the saturation density of stainless steel and partially scrubbed copper is comparable. This suggests that improvements in electron cloud performance by using copper only last until the copper gets scrubbed by the proton beam during commissioning or operation.

## CONCLUSION

We have presented the current estimate for electron cloud density and its impact for one of the proton beams of the JLEIC design. Though a more detailed estimate remains to

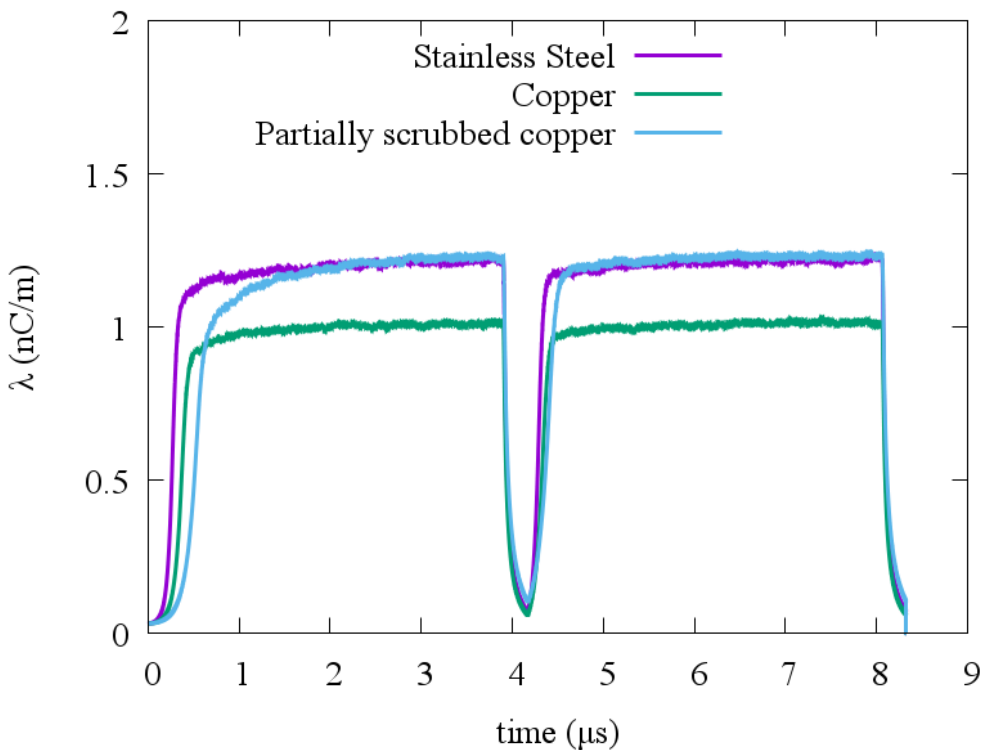


Figure 4: Electron cloud line density in a dipole as a function of time for two successive bunch trains for beam pipes of stainless steel, copper, and partially scrubbed copper.

Table 5: Simulation Results for Different Beam Pipe Materials

Element	$\lambda_e$ (nC/m)	$\rho_e$ (m <sup>-3</sup> )	$\Delta\nu_x$ (10 <sup>-3</sup> )	$\Delta\nu_y$ (10 <sup>-3</sup> )
Partially scrubbed copper	1.24	$1.54 \times 10^{12}$	1.21	1.63
Stainless steel	1.23	$1.53 \times 10^{12}$	1.20	1.62
Copper	1.02	$1.27 \times 10^{12}$	0.995	1.34

be done, an upper bound for the beam tune shift has been calculated and found to be reasonable. Future work is the evaluation of the electron cloud in other JLEIC collision schemes, in order to choose the correct material for the machine in all cases.

## ACKNOWLEDGEMENT

This material is based upon work supported by the U.S. Department of Energy, Office of Science, Office of Nuclear

Physics under contract DE-AC05-06OR23177. K. E. D. would like to thank LINAC'18 for conference support.

## REFERENCES

- [1] E. Gianfelice-Wendt, *ICFA Beam Dynamics Newsletter* No. 74, p. 92-182 (2018).
- [2] G. Iadarola, Electron cloud studies for CERN particle accelerators and simulation code development, Ph.D. thesis, Università degli Studi di Napoli Federico II, 2014.
- [3] T. Michalski, R. Fair, R. Rajput-Ghoshal, and P. Ghoshal, "JLEIC SC Magnets: Replace SF and High CM Energy Needs", (2018).
- [4] R. Valizadeh, O. B. Malyshev, S. Wang, S. A. Zolotovskaya, W. A. Gillespie, and A. Abdolvand, *Appl. Phys. Lett.* **105**, 231605 (2014).
- [5] R. Cimino *et al.*, *Phys. Rev. Lett.* **93**, 014801 (2004).